Table 2. *EMP3* expression in malignancies.

Tumor tissue				Cell line					Method	Ref.
Neuroblastoma	**Glioma**	**ESCC**	**Breast cancer**	**Neuroblastoma**	**Brain tumor**	**ESCC**	**Breast cancer**	**Lung cancer**		
							None 70% (14*/20)		Real-time RT-PCR	[21]
Ganglioneuroma				None 33% (3‡/9)	None 50% (1§/2)				Cell line: RT-PCR Tissue: microarray	[4]
	OG: low 20% (8/41), high 15% (6/41) OA: low 13% (2/16), high 31% (5/16)								Real-time RT-PCR	[20]
	OG: low 39% (12/31), high 26% (8/31) OA low 40% (4/10), high 40% (4/10) AC: low 21% (4/19), high 42% (8/19) pGBM low 0% (0/9), high 89% (8/9) sGBM low 0% (0/9), high 100% (9/9) pGBM > sGBM, AC								Real-time RT-PCR	[22]
	Glioblastoma: very high								Microarray	[26]
		Generally similar				Low 100% (20/20)	Low 75% (6/8)	Low 11% (1/9)	Real-time RT PCR (compared with normal tissue)	[3]
			Tumor > normal; higher in aggressive type; higher with HER2+						RT-PCR, real-time RT-PCR	[32]

*None: includes all non-invasive type cell lines.

‡None: CpG hypermethylated and *MYCN* amplified cell lines only.

§None: glioma cell line (The remaining was a medulloblastoma cell line).

AC: Astrocytoma and anaplastic astrocytoma; ESCC: Esophageal squamous cell carcinoma; HER2: Human EGF receptor 2; OA: Oligoastrocytoma and anaplastic oligoastrocytoma; OG: Oligodendroglioma and anaplastic oligodendroglioma; pGBM: Primary glioblastomas; sGBM: Secondary glioblastomas.

Table 3. *EMP3* promoter hypermethylation in malignancies.

Tumor tissue					Cell line						5-aza-dC treated cell line		Ref.
Neuroblastoma	Glioma	ESCC	Breast cancer	Phaeochromocytoma	Neuroblastoma	Brain tumor	ESCC	Breast cancer	Lung cancer	Method	EMP3 expression level	Method	
24% (28/116)	39% (16/41)				33% (3*/9)	50% (1‡/2)				MSP	Restored	MSP	[4]
	Oligodendroglial tumor: 90% (26/29)									Bisulfite sequence			[20]
	OG: 76% (44/58) OA 75% (12/16) AC: 84% (41/49) pGBM 17% (5/30) sGBM 89% (8/9)									Bisulfite sequence			[22]
68% (13/19)				6% (2/33)	Very frequent (?/10)					MSP	Up 1.61 – 2.94-fold restored	Microarray	[25]
		6% (1/17)					75% (15/20)	75% (6/8)	22% (2/9)	Quantitative MSP	Up 1.4 – 2.0-fold restored (still low)	Real-time RT PCR	[3]
			36.5% (23/63)							MSP			[32]

**MYCN* amplified cell lines only.

‡Glioma cell line (The remaining line was a medulloblastoma cell line).

AC: Astrocytoma and anaplastic astrocytoma; OA: Oligoastrocytoma and anaplastic oligoastrocytoma; OG: Oligodendroglioma and anaplastic oligodendroglioma; pGBM: Primary glioblastomas; sGBM: Secondary glioblastomas.

These findings indicate that the *EMP3* repression is related to malignant potential and regulated by promoter methylation in neuroblastoma.

3.2 Brain tumor

EMP3 has been reported to be hypermethylated in its promoter region and strongly repressed in a glioma cell line U-87, but not in a medulloblastoma cell line D283 [4].

For clinical samples, the *EMP3* CpG island hypermethylation evaluated by methylation-specific PCR analysis was reported to be found in 39.0% of glioma tissues (16 of 41) and no association was found with age of onset, sex, or histological types [4]. Li *et al.* reported that only 17.5% (10 of 57 cases) of oligodendroglial tumors showed reduced *EMP3* mRNA expression, 6 of them also carried a 19q13 deletion, and 19.3% (11 of 57 cases) showed enhanced expression, while 89.7% (26 of 29 cases examined) showed aberrant methylation of the CpG sites independent of the expression levels, indicating that methylation alone does not mediate transcriptional downregulation of *EMP3* in oligodendroglial tumors [20]. Reduced *EMP3* expression was frequently accompanied with deletion of 1p36 and/or 19q13, while enhanced expression never was.

Kunitz *et al.* reported that 16 of 41 oligodendroglial tumors (39%) but only 4 of 37 astrocytic tumors (11%) exhibited reduced *EMP3* mRNA levels by at least 50% relative to non-neoplastic brain tissue [22]. The *EMP3* expression levels were lower in oligodendroglial tumors with allelic losses on 19q compared with those without losses ($p = 0.01$), but were similar in astrocytic tumors. The *EMP3* mRNA expression was significantly higher in primary glioblastoma multiforme when compared with either secondary glioblastoma multiforme ($p = 0.008$), diffuse astrocytoma WHO grade II (AII) ($p = 0.005$), or anaplastic astrocytoma WHO grade III (AIII) ($p = 0.009$) [22]. Although *EMP3* overexpression in primary glioblastomas compared with non-neoplastic white matter tissue was confirmed also by others [26], there is no information yet on this upregulation of EMP3 expression in primary glioblastoma multiforme. Unexpectedly, it was demonstrated that the *EMP3* hypermethylation was associated with longer overall survival in the 46 patients with oligodendroglial tumors ($p = 0.0323$) by univariable analysis. However, multivariable analysis using Cox's proportional hazards regression model identified 1p/19q loss ($p = 0.04$), but not *EMP3* hypermethylation, as an independent indicator of better prognosis. Thus, the relationship of *EMP3* hypermethylation and favorable prognosis might not be due to the biological consequence of EMP3 inactivation but possibly due to the 1p and 19q losses which are frequently observed in combination and known as a favorable prognostic factor in oligodendrogliomas (reviewed in [27]). It was also reported that compared with benign ganglioneuromas, *EMP3* expression in gliomas was less than one-third [4], while it was significantly higher in glioblastomas [26].

3.3 Esophageal cancer

EMP3 was repressed in all 20 ESCC cell lines examined, 7 with CpG hypermethylation, 8 with partial methylation, and five of them without methylation [3]. Nevertheless, *EMP3* promoter methylation ratios calculated by quantitative MSP using fragment analysis and mRNA expression levels evaluated by real-time RT-PCR in ESCC cell lines were inversely correlated ($r = -0.73$, $p = 0.0002$). The *EMP3* repression was not sufficiently restored after demethylation by 5-azacytidine treatment. These findings indicated that not only CpG island hypermethylation but also other mechanisms must be involved in *EMP3* repression in ESCC [3]. Interestingly, the *EMP3* mRNA expression levels were inversely correlated with telomerase reverse-transcriptase gene (*TERT*) mRNA, in 20 ESCC cell lines ($r = -0.42$, $p = 0.065$) and *EMP3*-transfected clones (two and three clones each in two ESCC cell lines). Telomerase is a well known enzyme that can endow eukaryotic cells with extended lifespan or cellular immortality, by compensating for telomere shortening due to end-replication problems in cell division [28,29].

For clinical samples, the *EMP3* CpG island hypermethylation was partially detected in only one of 17 ESCC tissue samples (5.9%) and all the remaining cases showed no evidence of promoter hypermethylation evaluated by quantitative MSP using fluorescent primers, while mRNA expression level was low in one third cases [3]. Interestingly, in patients with advanced esophageal cancers who had received curative esophagectomy followed by 5 fluorouracil (5-FU)/ *cis*-diamminedichloroplatinum (CDDP) combination chemotherapy, disease specific survival rate after recurrence was significantly poorer in ESCC cases with low *EMP3* expression compared with those with high expression ($p = 0.05$), while disease-free survival (DFS) was similar in the two groups [3]. This finding indicates that suppression of *EMP3* may not provide growth advantage in early stages but works in late stages. This finding seems similar to the prognosis in neuroblastoma, as the promoter hypermethylation in *EMP3* is related to long-term prognosis of patients after 2 years survival [4].

3.4 Breast cancers

EMP3 mRNA was reported to be completely repressed in 14 of 20 breast cancer cell lines, including all 12 non-invasive phenotype (less ability to penetrate into a collagen-fibroblast matrix, many of them with estrogen receptor and progesterone receptor but not plasminogen activator inhibitor-1 expression) [21]. Interestingly, *EMP3* was identified as candidates of invasive type-specifically overexpressed genes with the other members of the transmembrane glycoprotein family, *EMP1* and *PMP22*. We also found the *EMP3* mRNA repression in six of eight breast cancer cell lines (75%), five lines were overlapped with the above, and all these six cell lines had CpG methylation [3]. Thus, *EMP3* repression is probably caused by CpG hypermethylation in almost all the noninvasive phenotype and a part of the invasive phenotype

breast cancer cell lines. In addition, it was reported that *EMP3* expression, as well as that of *EMP1*, was significantly upregulated in *ERBB2* (HER2/*neu*) transfectants of human mammary luminal epithelial cells in an expression-level-dependent manner [30]. Since *ERBB2* overexpression has been reported to be associated with poor prognosis, and resistance to both chemotherapy and endocrine therapy [31], above findings indicate that EMP3 repression might be involved in breast cancers only with low-malignant phenotype, and it may be upregulated in others. Also in clinical samples, Zhou *et al.* reported that the expression levels of *EMP3* mRNA in primary breast carcinomas were significantly higher than those in normal breast tissues ($p < 10^{-7}$), and significantly related to aggressive phenotypes such as histological grade III, lymph node metastasis, and strong human EGF receptor 2 (Her-2) expression [32]. The biological meaning of *EMP3* upregulation is discussed in 'Expert opinion', but remains to be confirmed.

3.5 Other malignancies

We also found *EMP3* mRNA repression in only one of nine lung cancer cell lines (11%) with partial CpG methylation, and the remaining eight lung cancer cell lines and both gastric- and all four colon-cancer-derived cell lines examined showed high expression [3]. These findings indicate that *EMP3* repression in cancers is organ-specific phenomenon, common in esophageal cancer, relatively common in neuroblastoma, glioma and breast cancer, and rare in lung, gastric, and colon cancer cell lines. In other tumor tissues, the hypermethylation of the *EMP3* CpG island in pheochromocytoma was reported to be rare, only in 2 of 33 cases (6.1%), independent of sporadic or VHL-associated cases [25].

3.6 Normal cell/tissues

In all normal tissues analyzed, including lymphocytes, adrenal medulla tissues [4], esophageal tissues, bronchial epithelial cells, mammary cells, fibroblasts [3], and brain tissues [20,22], the *EMP3* CpG island was completely unmethylated without mRNA repression. These findings also support the role of *EMP3* as a tumor suppressor gene.

4. *EMP3* as a tumor suppressor gene

Whereas some controversial findings are observed in breast cancers and gliomas, various pieces of evidence of *EMP3* as a tumor suppressor gene have been accumulated. The reintroduction of *EMP3* into deficient neuroblastoma cell lines induced tumor suppressor-like features, such as reduced colony formation density ($p < 0.001$) *in vitro* and tumor growth ($p < 0.001$) in nude mouse xenograft models [4]. Transfection of *EMP3* into HEK-293 cells, transformed human embryonic kidney cells, induced cell blebbing and annexin V binding resulting in cell death through the caspase-dependent pathway [18]. We also found that transfection of *EMP3* into esophageal squamous cell carcinoma (ESCC) cell lines induced low cloning efficacy and growth inhibition, in proportion to their EMP3 expression levels (Figure 1, A – C) with enhanced contact inhibition and morphological changes (enlarged and flattened) in some population among the small cells retaining original morphology (Figure 1, D) [3].

5. Regulation mechanism of *EMP3* expression

5.1 Methylation of the *EMP3* promoter region

As summarized in Table 3, *EMP3* CpG island hypermethylation is frequently observed in neuroblastoma, gliomas, esophageal squamous cell carcinoma (cell lines), and breast cancer (cell lines), and much less frequently in pheochromocytoma and lung cancer (cell lines), while it has never beeen observed in normal tissues or cells. In oligodendroglial tumors, *EMP3* mRNA levels were significantly lower ($p = 0.006$) and more commonly reduced ($p = 0.03$) in tumors with *EMP3* hypermethylation when compared with tumors without *EMP3* hypermethylation [22]. Similarly, *EMP3* hypermethylation in astrocytic gliomas was significantly associated with lower transcript levels ($p = 0.005$) [22]. We also reported an inverse relationship between promoter methylation ratios and mRNA expression levels in ESCC cell lines [3]. The repressed mRNA levels were restored qualitatively [4] or quantitatively from 1.61- to 2.94-fold [25] in neuroblastoma cell lines and 1.40- and 2.01-fold in ESCC cell lines [3] by 5-azacytidine treatment. So, there is no doubt that methylation of the *EMP3* promoter region is a major mechanism of EMP3 inactivation. However, in ESCC cell lines, *EMP3* mRNA expression was repressed even without promoter methylation and the restoration by 5-azacytidine treatment in hypermethylated cell lines was insufficient [3]. In oligodendroglial tumors, no correlation was observed between transcript level and methylation status in one report [20], whereas it was observed by Kunitz *et al.* [22], indicating that additional *EMP3* silencing mechanisms exist in these tumors, while all *EMP3* repressed samples were accompanied with promoter methylation in breast cancer cell lines [3].

5.2 Deletion/loss of heterozygosity (LOH)

A significant relationship between the 19q deletion/LOH and *EMP3* mRNA repression has been found in oligodendroglial tumors ($p = 0.01$) [22] and one with *EMP3* promoter hypermethylation was observed in oligodendroglial tumors ($p = 0.02 - < 0.001$ according to histology) [22] and neuroblastoma ($p = 0.004$) [4]. In contrast, overexpression of *EMP3* was significantly associated with balanced 19q13 ($p = 0.002$) [20]. Thus, deletion of the *EMP3* locus may be one of the important mechanisms of *EMP3* inactivation.

5.3 *EMP3* genetic variation

In the 132 gliomas, two constitutional single nucleotide substitutions, rs4893 (missense mutation Ile125Val) and rs11671746 (3'UTR) were detected in exon 5 in four patients whereas no tumor-specific mutation was found in

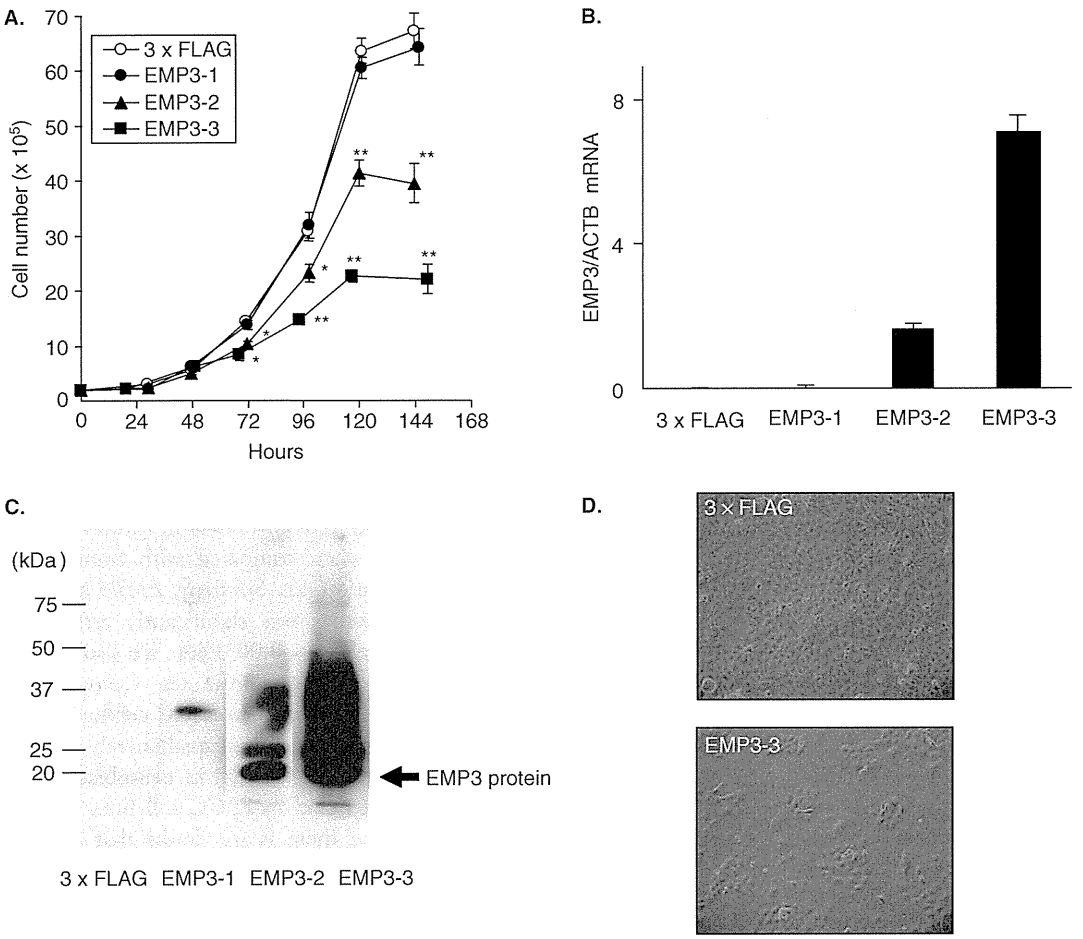

Figure 1. Effects of EMP3 overexpression in ESCC cell line KYSE170 [3]. EMP3 transfected clones EMP3-1, -2, and -3 showed growth inhibition (A) according to their mRNA (B) or protein (C) expression levels, compared to the control clone transfected with the control vector 3 × FLAG. Cell numbers in culture started from 2×10^5 in a 10 cm dish are expressed as mean ± SD in triplicate experiments (A). *P < 0.01, **P < 0.001. The *EMP3* mRNA level was evaluated by real-time RT-PCR (B, mean + SD). EMP3 protein amount was evaluated by Western blotting using anti-FLAG M2 as the primary antibody (C, arrow) The EMP3 overexpressing clones EMP3-3 showed morphological changes, being enlarged and flattened, and growth inhibition, compared with the control clone 3 × FLAG (D).

the *EMP3* coding region [22]. The rs4893 variant allele had been reported to be more frequently observed in prostate cancer patients (0.045) than in controls (0.013, $p < 0.0001$) [33], but this low allele frequency indicates that this missense mutation cannot be the major mechanism of EMP3 inactivation. We also investigated the genetic variations in possible promoter regions and the coding regions in ESCC, colon and lung cancer cell lines and tissues principally with low and high *EMP3* expression levels, respectively, and found no tumor-specific mutations that explain the dysregulation of this gene expression [3]. The rs4893 single nucleotide polymorphisms (SNPs) in exon 5 was found only in a lung cancer cell line A549 among 46 individuals examined. We also found a Japanese- or Asian-population-specific haplotype of three SNPs (rs8102349, rs8355 and rs11665, **Figure 2**) in non-coding regions or introns with variant allele frequency 0.28, but no association was found with the *EMP3* expression levels [3]. Thus, genetic variation is unlikely to contribute to *EMP3* inactivation.

5.4 Unidentified repressor

We found that 24-h treatment with trichostatin A (TSA), which inhibits histone deacetylase (HDAC), induced dramatic repression of the *EMP3* mRNA expression in a dose-dependent manner in all HEEC-1 non-cancerous esophageal epithelial cells and ST11 and TF-1 *in vitro* immortalized fibroblast cell lines that originally had no repression. Meanwhile, no effect was observed in originally *EMP3*-repressed ESCC cell lines and a hepatocarcinoma cell line HepG2 regardless of the promoter hypermethylation status [3]. These findings indicate that there may be a repressor of *EMP3* that is regulated by HDAC in EMP3 expressing cells but active

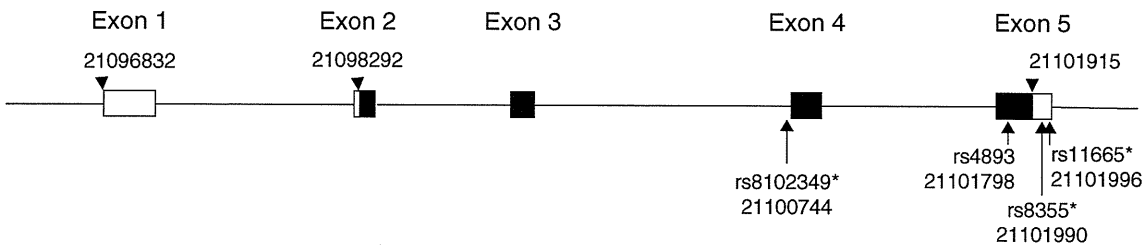

Figure 2. Representative polymorphisms in the *EMP3* gene. Locations of initiation sites of transcription and translation, stop codons (arrowheads), and representative polymorphisms (arrows) are numbered according to the contig positions and rs numbers are cluster IDs registered in dbSNP [35]. Closed box: coding exon, Open boxes: untranslated exon.
*Haplotype found in Japanese [3].

in EMP3-repressed cells without promoter hypermethylation such as ESCC cells. However, the existence of this repressor remains to be elucidated.

6. Prognostic marker

In neuroblastoma, it was reported that *EMP3* is a good candidate for being the long-sought tumor suppressor gene because *EMP3* promoter hypermethylation was significantly associated with poor survival after the first 2 years of onset of the disease ($p = 0.05$) and death from disease ($p = 0.03$) [4]. Similarly, when the ESCC patient prognosis was compared with the *EMP3* expression level, low *EMP3* expression was associated with poor prognosis after recurrence ($p = 0.05$), whereas it was not associated with DFS [3]. However, in oligodendroglial tumors, the *EMP3* hypermethylation as well as the 1p/19q losses were favorable prognosis factors [22]. Further, the most malignant phenotype of gliomas, glioblastoma multiforme, were revealed to have enhanced expression of *EMP3* in all samples examined. In addition, Zhou *et al.* recently reported that *EMP3* overexpression in breast carcinomas was correlated with carcinoma aggressiveness [32]. To explain these discrepancies, we considered that there might be an EMP3-independent factor(s) that promote cellular immortalization in particular malignancies, as proposed in Figure 3 and discussed below.

7. Expert opinion

EMP3, located on chromosome 19q13 [8], has been implicated as a candidate tumor suppressor gene for some solid tumors such as neuroblastoma, glioma and ESCC, with reliable studies using *EMP3* overexpression and knockdown experiments [3,4]. Furthermore, the high frequency of CpG island methylation in ESCC cell lines but not in ESCC tissues, inverse relationship between *EMP3* and *TERT* expression levels in ESCC cell lines, ESCC tissues and *EMP3* transfectants, positive relationship of *EMP3* repression with poor prognosis after recurrence (disease-specific survival (DSS)-DFS) but not with that until recurrence (DFS) in ESCC patients [3], and positive relationship of *EMP3* promoter methylation with poor prognosis after 2-year survival but not in overall prognosis of patients with neuroblastoma [4] indicated that the inactivation of *EMP3* may promote cellular immortalization with telomerase activation in such cancer cells. Tumor tissues may contain certain amounts of mortal cancer cells without telomerase expression while all cells in cell lines are immortal [34], this would explain the difference of *EMP3* methylation frequency between the ESCC cell lines and tissues. Although the tissue heterogeneity of clinical samples may have contributed to a part of this difference, the findings that no tissue sample showed high methylation rate nor absence of expression indicate that it may have derived from the biological difference between tissue samples and cell lines, that is existence of mortal cells or not. Before recurrence, cancer cells have not experienced so many cell divisions to critically shorten their telomeres, explaining the absence of effect of cellular immortalization on DFS, but after recurrence only immortalized cancer cells with telomerase activation could continue to proliferate resulting in short DSS-DFS. However, we speculate that there might be an EMP3-independent factor(s), possibly stronger than EMP3, that promote cellular immortalization in particular malignancies, for example glioblastoma multiforme, aggressive type oligodendroglial tumors, gastric cancer, colon cancer, lung cancer (majority), and invasive phenotype mammary carcinoma cell lines, but not in neuroblastoma and ESCC. If this putative factor exists in a tumor, EMP3 inactivation does not endow these cells with a growth advantage any more, then no promoter methylation nor repression may occur, and on the contrary as an innate inhibitory mechanism of cellular immortalization, *EMP3* might be overexpressed in such tumors (Figure 3). If such an EMP3-independent immortalization promoting factor is the dominant adverse prognostic event, then *EMP3* promoter methylation or 1p/19q losses may correlate with good prognosis in gliomas [22], and *EMP3* expression may be enhanced only in invasive-type breast cancer cell lines and upregulated in *ERBB2* (HER2/*neu*) transfectants of human mammary luminal epithelial cells [30]. In fact, *EMP3* expression levels in almost all of ESCC (20/20) and many breast cancer (20/28) cell lines

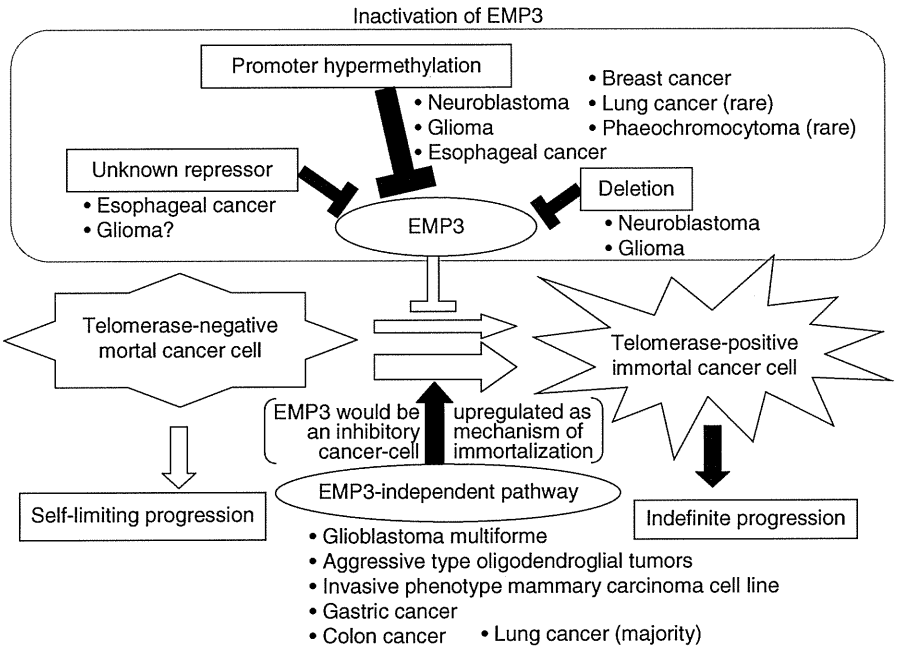

Figure 3. Hypothetical regulation and function of EMP3 in human malignancies (authors' speculation). EMP3 may have an inhibitory role in cellular immortalization of neuroblastoma, glioma, and esophageal cancers, while some EMP3-independent pathway(s) might exist in glioblastoma, aggressive type oligodendroglioma, invasive phenotype mammary carcinoma, gastric cancer, and colon cancer.

were lower than those of non-cancerous strains, but were only in a few lung cancer cell lines (1/9) [3,4]. Meanwhile in tissue samples, *EMP3* expression levels in glioblastoma and breast cancer tissues are higher than those of non-cancerous tissues, but not in ESCC or neuroblastoma [3,4,26,32]. These findings can be explained by our above hypothesis that EMP3 acts as a tumor suppressor gene in various tumors at the cellular immortalization step, but there may be another EMP3-independent pathway for cellular immortalization in particular malignancies, for example, glioblastoma multiforme and breast cancer, but not in ESCC and neuroblastoma (Figure 3).

In conclusion, EMP3 may act as a tumor suppressor in some kinds of malignancies, neuroblastoma and ESCC but not all, at the step of cellular immortalization rather than the step of carcinogenesis. As for the regulation mechanism of *EMP3* expression, allele loss and/or promoter hypermethylation are relatively common, but also an unidentified repressor(s) that is regulated by HDAC may exist at least in ESCC. Genetic mutation is unlikely to be the major mechanism of EMP3 inactivation. Although there are black boxes to be elucidated, *EMP3* can be a potent prognostic marker for some types of solid tumors and allow us to develop a novel molecular targeting therapy in future.

Declaration of interest

The authors state no conflict of interest and have received no payment in preparation of this manuscript.

Bibliography

Papers of special note have been highlighted as either of interest (•) or of considerable interest (••) to readers.

1. Brenton JD, Carey LA, Ahmed AA, Caldas C. Molecular classification and molecular forecasting of breast cancer: ready for clinical application? J Clin Oncol 2005;23(29):7350-60
2. Konstantinopoulos PA, Spentzos D, Cannistra SA. Gene-expression profiling in epithelial ovarian cancer. Nat Clin Pract Oncol 2008;5(10):577-87
3. Fumoto S, Hiyama K, Tanimoto K, et al. EMP3 as a tumor suppressor gene for esophageal squamous cell carcinoma. Cancer Lett 2009;274(1):25-32

•• **The first paper, to our knowledge, that demonstrated the inactivation of EMP3 in digestive organ-derived malignancies (esophageal cancer), and the authors proposed that it regulates the late step of carcinogenesis and is inactivated by some unidentified repressor, as well as promoter hypermethylation.**

4. Alaminos M, Davalos V, Ropero S, et al. EMP3, a myelin-related gene located in the critical 19q13.3 region, is epigenetically silenced and exhibits features of a candidate tumor suppressor in glioma and neuroblastoma. Cancer Res 2005;65(7):2565-71

•• **The first paper, to our knowledge, that proposed the possibility of *EMP3* being a tumor suppressor gene in neuroblastoma and glioma, demonstrating frequent hypermethylation of the *EMP3* promoter in them.**

5. Ben-porath I, Benvenisty N. Characterization of a tumor-associated gene, a member of a novel family of genes encoding membrane glycoproteins. Gene 1996;183(1-2):69-75

• **The authors cloned the human *EMP3* (named as *YMP*) as well as *EMP1* (*TMP*) and *EMP2* (*XMP*) independently of Taylor *et al.* [7] and found an inverse reaction between *PMP22* and *EMP1*.**

6. Taylor V, Suter U. Epithelial membrane protein-2 and epithelial membrane protein-3: two novel members of the peripheral myelin protein 22 gene family. Gene 1996;175(1-2):115-20
7. Taylor V, Welcher AA, Program AE, Suter U. Epithelial membrane protein-1, peripheral myelin protein 22, and lens membrane protein 20 define a novel gene family. J Biol Chem 1995;270(48):28824-33

• **The first paper, to our knowledge, reporting cloning of *EMP3* as well as *EMP2*, and demonstrated their expression distribution in adult and fetal organs.**

8. Liehr T, Kuhlenbaumer G, Wulf P, et al. Regional localization of the human epithelial membrane protein genes 1, 2, and 3 (EMP1, EMP2, EMP3) to 12p12.3, 16p13.2, and 19q13.3. Genomics 1999;58(1):106-8
9. Ben-Porath I, Kozak CA, Benvenisty N. Chromosomal mapping of Tmp (Emp1), Xmp (Emp2), and Ymp (Emp3), genes encoding membrane proteins related to Pmp22. Genomics 1998;49(3):443-7
10. Jetten AM, Suter U. The peripheral myelin protein 22 and epithelial membrane protein family. Prog Nucleic Acid Res Mol Biol 2000;64:97-129

• **Review of the PMP22/EMP family that includes a description of EMP3.**

11. Bolin LM, McNeil T, Lucian LA, et al. HNMP-1: a novel hematopoietic and neural membrane protein differentially regulated in neural development and injury. J Neurosci 1997;17(14):5493-502
12. Fabbretti E, Edomi P, Brancolini C, Schneider C. Apoptotic phenotype induced by overexpression of wild-type gas3/PMP22: its relation to the demyelinating peripheral neuropathy CMT1A. Genes Dev 1995;9(15):1846-56
13. Snipes GJ, Suter U, Shooter EM. Human peripheral myelin protein-22 carries the L2/HNK-1 carbohydrate adhesion epitope. J Neurochem 1993;61(5):1961-4
14. Gnirke AU, Weidle UH. Investigation of prevalence and regulation of expression of progression associated protein (PAP). Anticancer Res 1998;18(6A):4363-9
15. Marvin KW, Fujimoto W, Jetten AM. Identification and characterization of a novel squamous cell-associated gene related to PMP22. J Biol Chem 1995;270(48):28910-6
16. Chance PF. Inherited focal, episodic neuropathies: hereditary neuropathy with liability to pressure palsies and hereditary neuralgic amyotrophy. Neuromolecular Med 2006;8(1-2):159-74
17. Zucchi I, Montagna C, Susani L, et al. Genetic dissection of dome formation in a mammary cell line: identification of two genes with opposing action. Proc Natl Acad Sci USA 1999;96(24):13766-70
18. Wilson HL, Wilson SA, Surprenant A, North RA. Epithelial membrane proteins induce membrane blebbing and interact with the P2X7 receptor C terminus. J Biol Chem 2002;277(37):34017-23

• **The first paper, to our knowledge, that demonstrated the evidence that overexpression of *EMP3*, or either of the PMP22/EMP family members, induced apoptosis pathway in transformed kidney cells.**

19. Li Z, Srivastava S, Yang X, et al. A hierarchical approach employing metabolic and gene expression profiles to identify the pathways that confer cytotoxicity in HepG2 cells. BMC Syst Biol 2007;1:21 [published online 11 May 2007]
20. Li KK, Pang JC, Chung NY, et al. EMP3 overexpression is associated with oligodendroglial tumors retaining chromosome arms 1p and 19q. Int J Cancer 2006;120(4):947-50
21. Evtimova V, Zeillinger R, Weidle UH. Identification of genes associated with the invasive status of human mammary carcinoma cell lines by transcriptional profiling. Tumour Biol 2003;24(4):189-98

• **The authors demonstrated contrasting findings that EMP3 was associated with invasive phenotype in human mammary carcinoma cell lines.**

22. Kunitz A, Wolter M, van den Boom J, et al. DNA hypermethylation and aberrant expression of the EMP3 gene at 19q13.3 in human gliomas. Brain Pathol 2007;17(4):363-70

•• **The authors analyzed precisely EMP3 expression, methylation, and deletion in gliomas and demonstrated an opposite association with prognosis (EMP3 inactivation was a favorable marker).**

23. Hiyama E, Hiyama K, Ohtsu K, et al. Telomerase activity in neuroblastoma: is it a prognostic indicator of clinical behaviour? Eur J Cancer 1997;33(12):1932-6
24. Riley RD, Heney D, Jones DR, et al. A systematic review of molecular and biological tumor markers in neuroblastoma. Clin Cancer Res 2004;10(1 Pt 1):4-12
25. Margetts CD, Morris M, Astuti D, et al. Evaluation of a functional epigenetic approach to identify promoter region methylation in phaeochromocytoma and neuroblastoma. Endocr Relat Cancer 2008;15(3):777-86

26. Scrideli CA, Carlotti CGJ, Okamoto OK, et al. Gene expression profile analysis of primary glioblastomas and non-neoplastic brain tissue: identification of potential target genes by oligonucleotide microarray and real-time quantitative PCR. J Neurooncol 2008;88(3):281-91
27. Jaeckle KA, Ballman KV, Rao RD, et al. Current strategies in treatment of oligodendroglioma: evolution of molecular signatures of response. J Clin Oncol 2006;24(8):1246-52
28. Shay JW, Wright WE. Telomerase therapeutics for cancer: challenges and new directions. Nat Rev Drug Discov 2006;5(7):577-84
29. Hiyama K, Hiyama E, Shay JW. Telomeres and telomerase in humans. In: Hiyama K, editor. Telomeres and telomerase in cancer. Humana Press: Springer, New York. 2009. p. 3-21
30. Mackay A, Jones C, Dexter T, et al. cDNA microarray analysis of genes associated with ERBB2 (HER2/neu) overexpression in human mammary luminal epithelial cells. Oncogene 2003;22(17):2680-8
31. Prat A, Baselga J. The role of hormonal therapy in the management of hormonal-receptor-positive breast cancer with co-expression of HER2. Nat Clin Pract Oncol 2008;5(9):531-42
32. Zhou W, Jiang Z, Li X, et al. EMP3 overexpression in primary breast carcinomas is not associated with epigenetic aberrations. J Korean Med Sci 2009;24(1):97-103
33. Burmester JK, Suarez BK, Lin JH, et al. Analysis of candidate genes for prostate cancer. Hum Hered 2004;57(4):172-8
- **The only report, to our knowledge, that demonstrated a positive association of *EMP3* genetic variation (rs4893) with cancer susceptibility.**
34. Hiyama K, Hiyama E, Ishioka S, et al. Telomerase activity in small-cell and non-small-cell lung cancers. J Natl Cancer Inst 1995;87(12):895-902
35. dbSNP (NCBI Single Nucleotide Polymorphism database), Available from: http://www.ncbi.nlm.nih.gov/sites/entrez?db=snp [last accessed 28 April 2009]
36. Available from: http://www.ncbi.nlm.nih.gov/sites/entrez?db=gene: Gene (NCBI, gene database)
37. Available from: http://www.ncbi.nlm.nih.gov/sites/entrez?db=OMIM: OMIM (NCBI, Online Mendelian Inheritance in Man)
38. Available from: http://www.expasy.ch/sprot/sprot-top.html: Swiss-Prot (Swiss Institute of Bioinformatics, Protein knowledgebase)

Affiliation

Shoichi Fumoto[1,5] MD PhD,
Keiji Tanimoto[1] DDS PhD,
Eiso Hiyama[2] MD PhD,
Tsuyoshi Noguchi[3] MD PhD,
Masahiko Nishiyama[1,4] MD PhD &
Keiko Hiyama[†1] MD PhD
[†]Author for correspondence
[1]Hiroshima University,
Research Institute for Radiation Biology and Medicine (RIRBM),
Department of Translational Cancer Research,
Hiroshima, 734-8551, Japan
Tel: +81 82 257 5841; Fax: +81 82 256 7105;
E mail: khiyama@hiroshima-u.ac.jp
[2]Hiroshima University,
Natural Science Center for Basic Research and Development (N-BARD),
Hiroshima, 734-8551, Japan
[3]Faculty of Medicine
Oita University,
Department of Gastrointestinal Surgery,
Oita, 879-5593, Japan
[4]Saitama Medical University
International Medical Center,
Saitama, 350-1298, Japan
[5]Hiroshima University,
Graduate School of Biomedical Sciences,
Division of Clinical Oncology,
Hiroshima, 734-8551, Japan

Molecular Genetics and Metabolism 97 (2009) 292–296

Contents lists available at ScienceDirect

Molecular Genetics and Metabolism

journal homepage: www.elsevier.com/locate/ymgme

Fluctuating liver functions in siblings with MPV17 mutations and possible improvement associated with dietary and pharmaceutical treatments targeting respiratory chain complex II

Shunsaku Kaji [a,*,1], Kei Murayama [b,1], Ikuo Nagata [c], Hironori Nagasaka [b], Masaki Takayanagi [b], Akira Ohtake [d], Hiroyasu Iwasa [e,f], Masahiko Nishiyama [e], Yasushi Okazaki [f], Hiroko Harashima [d], Takahiro Eitoku [a], Michiko Yamamoto [a], Hiroaki Matsushita [a], Koichi Kitamoto [a], Shinji Sakata [a], Takeshi Katayama [a], Shuji Sugimoto [a], Yoshio Fujimoto [a], Jun Murakami [c], Susumu Kanzaki [c], Kazuo Shiraki [c]

[a] Department of Pediatrics, Tsuyama Central Hospital, Japan
[b] Department of Metabolism, Chiba Children's Hospital, Japan
[c] Division of Pediatrics & Perinatology, Faculty of Medicine, Tottori University, Japan
[d] Department of Pediatrics, Faculty of Medicine, Saitama Medical University, Japan
[e] Translational Research Center, International Medical Center, Saitama Medical University, Japan
[f] Division of Translational Research, Research Center for Genomic Medicine, Saitama Medical University, Japan

ARTICLE INFO

Article history:
Received 10 March 2009
Received in revised form 27 April 2009
Accepted 27 April 2009
Available online 12 May 2009

Keywords:
MPV17 mutations
Mitochondrial DNA depletion syndrome
Liver dysfunction
Viral infection
Mitochondrial respiratory chain complex
Succinate
Ubiquinone
Ketone milk
Lipid-rich diet
Treatment

ABSTRACT

Background/aims: To describe the clinical and biological findings of two Japanese siblings with novel MPV17 gene mutations (c.451insC/c.509C > T) manifesting hepatic mitochondrial DNA depletion syndrome.
Methods: We observed these brothers and sought to determine the efficacy of treatment targeting respiratory chain complex II for the younger brother.
Results: A 3-month-old boy had presented with profound liver dysfunction, failure to thrive, and watery diarrhea. Although he was then placed on a carbohydrate-rich diet, his liver function thereafter fluctuated greatly in association with viral infections, and rapidly deteriorated to liver failure. He underwent liver transplantation at 17 months of age but died at 22 months of age. The younger brother, aged 47 months at the time of this writing, presented with liver dysfunction from 8 months of age. His transaminase levels also fluctuated considerably fluctuations in association with viral infections. At 31 months of age, treatment with succinate and ubiquinone was initiated together with a lipid-rich diet using ketone milk. Thereafter, his transaminase levels normalized and never fluctuated, and the liver histology improved.
Conclusions: These cases suggested that the clinical courses of patients with MPV17 mutations are greatly influenced by viral infections and that dietary and pharmaceutical treatments targeting the mitochondrial respiratory chain complex II may be beneficial in the clinical management of MPV17 mutant patients.

Introduction

MPV17 is a mitochondrial gene encoded by a nuclear gene [1]. Its mutations cause mitochondrial DNA depletion syndrome (MDS)[2], presenting multiple mitochondrial respiratory chain depletions in the manner of autosomal recessive inheritance [1–5]. Recently, the occurrence of patients with MPV mutations has been increasing; the majority of patients have developed liver disease within a few months after birth, with rapid deterioration to liver failure, while the remaining patients have shown relatively slow progression of liver disease or neurological regression [1–5].

However, the number of patients with MPV17 mutations is still small, and the clinical courses according to the mutations or the genotype- phenotype correlation remain unclear. Further, the appropriate internal therapy has yet to be established, although Parini and colleagues recently reported that glucose administration to avoid hypoglycemia is efficient in slowing the progression of liver disease [5].

* Corresponding author. Department of Pediatrics, Tsuyama Central Hospital, Kawasaki 1756, Tsuyama-shi, Okayama 708-0841, Japan. Fax: +81 868 21 8205.
E-mail address: skaji@tvt.ne.jp (S. Kaji).

[1] These two authors equally contributed to this work.

[2] *Abbreviations used:* MDS, mitochondrial DNA depletion syndrome; RC, respiratory chain; Co I, complex I; Co II, complex II; Co III, complex III; Co IV, complex IV; CS, citrate synthase.

1096-7192/$ - see front matter © 2009 Elsevier Inc. All rights reserved.
doi:10.1016/j.ymgme.2009.04.014

In this report, we present the clinical courses of two siblings with novel mutations, c.451insC and c.509C > T, whose liver functions greatly fluctuated according to their respective viral infections. The beneficial effect of treatment targeting mitochondrial respiratory chain (RC) complex (Co) II, including succinate and coenzyme Q, is also described.

Patients and methods

Cases

Case 1: A Japanese boy born as the second child to unrelated healthy parents. Their first son is healthy. The second son, on the other hand, was born without any complications at 37 weeks of gestation age, and weighed 3060 g. At 3 months of age, he was referred to our hospital to receive precise examinations for failure to thrive, hypotonia, mild jaundice, and creamy stools. He had moderate head lag and incomplete head control. He maintained good eye contact and had a sociable smile; he had no seizures or clinical signs of peripheral neuropathy except for moderate hypotonia. Findings of brain computed tomography were normal. The liver was soft and palpated at 4.5 cm below the costal margin with no splenomegaly. Laboratory tests then showed elevated levels of serum bilirubin, total bile acid (TBA), transaminases, and gamma-glutamyl transpeptidase (GGT) as well as prolonged coagulation time (total bilirubin 4.2 mg/dl; direct bilirubin 2.7 mg/dl; TBA 362 μmol/L; GGT 178 IU/L; AST 173 IU/L; ALT 58 IU/L; hepaplastin time 38%). He had no episode of hypoglycemia (his blood glucose level was 65 mg/dl). Simultaneously, low body weight and height were prominent (body weight 4610 g, −2.7 SD; height, 59 cm, −1.8 SD). His plasma amino acid profile and urinary organic acid profile did not suggest any etiology for liver disease, but viral examinations detected an IgM cytomegalovirus (CMV)-specific antibody in the plasma. His liver functions thereafter are shown in Fig. 1 (upper panel).

A liver biopsy specimen obtained at 4 months of age showed moderate inflammatory cell infiltration with destroyed limiting plates and fibrosis in the portal tracts (Fig. S1A1). Two different types of degenerated hepatocytes were found: swollen hepatocytes containing lipid droplets of various sizes with occasional formation of multinuclear giant cells, and small, concentrated acidophilic hepatocytes. Bile plugs were noticed in the cytoplasm of hepatocytes and dilated canaliculi, consistent with the findings of cholestasis (Fig. S1A2).

Immediately during his first visit to our hospital, he was fed with medium-chain triglyceride (MCT) milk (100–105 kcal/kg/day; lipid 25%, carbohydrate 56.6%, protein 13.2%, eight times per day) and received fat-soluble vitamins. His liver dysfunction improved at 7 months of age when the cytomegalovirus-IgM antibody became undetectable. However, 1 month later, he began to frequently vomit, and tube feeding was initiated. Thereafter, he developed recurrent bouts of jaundice and elevations of transaminases accompanied by flu-like signs such as nasal discharge and cough, and his liver dysfunction deteriorated to liver failure with cirrhosis (Fig. S1B shows his liver histology at 15 months of age). He underwent a liver transplantation at 17 months of age but died of recurrent peritonitis and the resultant sepsis at 22 months of age. Afterward, the liver specimens obtained through the explantation, which histologically showed cirrhosis, were subjected to mitochondrial RC examinations when his younger brother received RC examinations.

Case 2: The younger brother of case 1 was born, 15 months after his elder brother died, without any complications at 40 weeks of gestation, with a weight of 3260 g. At the age of 8 months he was referred to our hospital with failure to thrive (height, 62 cm, −3.5 SD; weight 5.5 kg, −3.1 SD) and mild cholestasis. He could sit up alone, but could not crawl yet. He had no seizure and no clinical sign of peripheral neuropathy except for mild hypotonia. He could appropriately respond to changes in emotional content of social interaction. His liver and spleen were not palpated below the costal margin. Liver function tests then showed mild or moderate elevations of serum AST, ALT, GGT, and TBA levels (AST, 150 IU/L; ALT 40 IU/L; GGT, 82 IU/L; TBA 40 μmol/L). The coagulation tests had normal results. He had no episode of hypoglycemia (his blood glucose level was 64 mg/dl). His plasma lactate and pyruvate levels were slightly elevated (lactate, 2.2–3.3 mmol/L; pyruvate 0.1–0.2 mmol/L), but his cerebrospinal fluid lactate and pyruvate levels were entirely normal. His amino acid profile in blood and organic acid profile in urine showed no finding suggesting an etiology, and serological viral tests were all negative. Brain magnetic resonance imaging (MRI) was normal at 9 months of age. His liver functions thereafter are shown in Fig. 1 (lower panel).

Liver histology at 8 months of age displayed mild infiltration of inflammatory cells, fibrosis in the portal tracts, and various-sized lipid droplets in hepatocytes, comparable to the histological findings of his elder brother. He was placed on a carbohydrate-rich, lipid-poor diet using MCT milk (100 kcal/kg/day; lipid 25%, carbohydrate 56.6%, protein 13.2%, eight times per day by nasogastric tube) as his elder brother had been, and was treated with fat-soluble vitamins and ursodeoxycholic acid.

His liver dysfunction thereafter fluctuated as a result of upper respiratory infections, probably due to some viruses, and diarrhea due to rotavirus infection (Fig. 1, lower panel).

Liver histology at 30 months of age showed a rather progressive fibrosis with bridging formation and inflammatory cell infiltration compared with that of the previous biopsy (Fig. S1C). The activity levels of mitochondrial RC Co I and III were decreased in this liver sample, whereas Co II activity remained normal (Table 1). Quantitative PCR revealed a decrease in the amount of mitochondrial DNA, and the boy was diagnosed with MDS. Gene analysis revealed that he is a compound heterozygote for mutations in the MPV17 gene responsible for MDS.

At 31 months of age, he began medication with carnitine (300 mg/day), succinate (2 g/day), and ubiquinone (coenzyme Q10: 30 mg/day). Simultaneously, the carbohydrate-rich, lipid-poor diet using MCT milk was changed to a lipid-rich, carbohydrate-poor diet using ketone milk (lipid 71.8%, carbohydrate 8.8%, protein 15%) and MCT milk (total: 90–100 kcal/kg/day; lipid 56.3–60.1%, carbohydrate 20.8–24.6%, protein 14.4–14.6%, eight times per day by nasogastric tube). After the initiation of these dietary and pharmaceutical treatments, his transaminases decreased to normal (Fig. 1, lower panel).

At the age of 37 months, a liver needle biopsy was again performed; infiltration by inflammatory cells decreased and fibrosis was suppressed, but fatty degeneration remained unchanged (Fig. S1D).

Recently, his body weight and height have increased gradually but are still low (body weight 10.3 kg, −2.6 SD; height 81.5 cm, −4.5 SD). Brain MRI was normal at 42 months of age. At the time of this writing, he is 47 months old, and shows normal psychomotor development.

Materials and methods

Samples for the examination of respiratory chains

The liver sample from the elder brother was the excised part of the liver transplantation at 17 months of age. Liver samples from the younger brother were obtained by liver biopsies at 30 and 37 months of age.

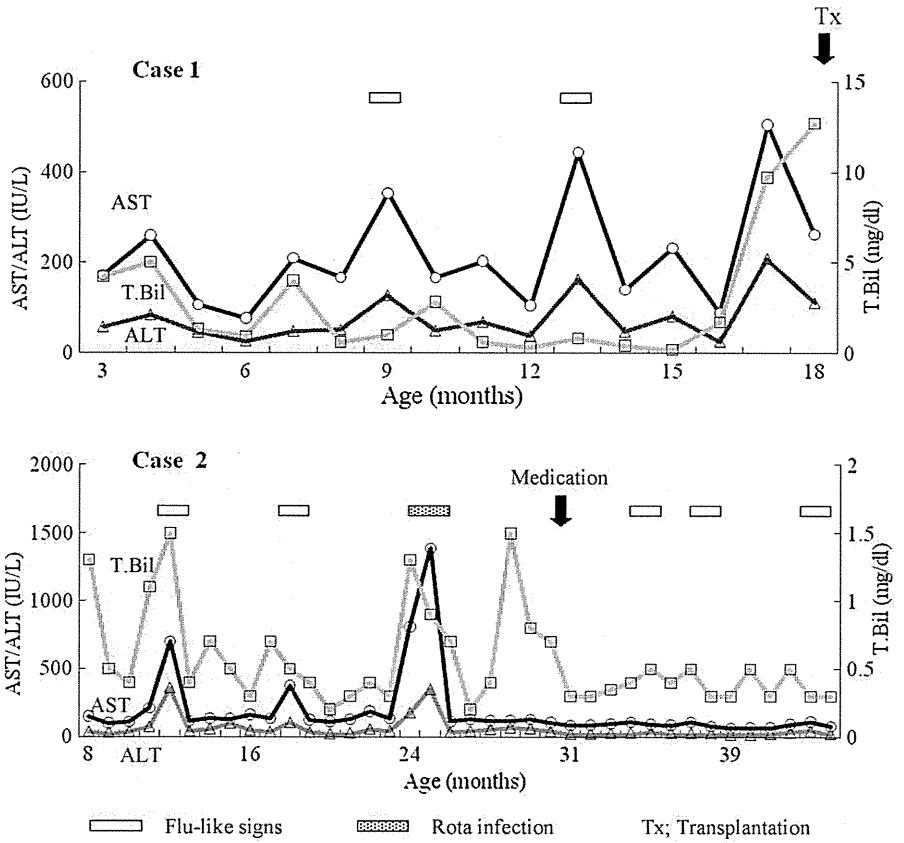

Fig. 1. Clinical courses of cases 1 (upper panel) and 2 (lower panel).

Determination of enzyme activities

Activities of RC Co I, II, III, and IV were assayed for the crude post-600 g supernatant of the liver samples as described previously [6,7]. The activity of each complex was presented as a percentage of the mean value obtained from 35 healthy controls. For each patient, the percentages of Co I, II, III, and IV activities relative to that of citrate synthase (CS) as a mitochondrial enzyme marker or Co II activity were calculated [6].

BN-PAGE Western blotting

Expression levels of the mitochondrial RC Co I, II, III, and IV proteins in the liver were examined by Western blotting using blue native polyacrylamide gel electrophoresis (BN-PAGE) according to the methods described previously [8,9]. Ten micrograms of the protein in the mitochondria-enriched fraction was separated by BN-PAGE. Immunostaining was performed using a monoclonal antibody specific for the 39 kD subunit of Co I, the 70 kD subunit of Co II, the core 1 subunit of Co III, and the subunit 1 of Co IV (Molecular Probes, Eugene, OR).

Quantitative PCR

mtDNA was quantitatively estimated by the real-time amplification of fragments of ND1 in the mtDNA genome, as previously described [10,11]. To determine the overall abundance of mtDNA, we compared the real-time amplification of ND1 with a single-

Table 1
Enzyme assay of respiratory chain and quantitative mtDNA evaluation by qPCR.

%	Co I	Co II	Co III	Co IV	CS	mtDNA/nDNA (%)
Elder Brother (17 months)						7.8
% of normal	0	80	13	41	300	
CS ratio	0	27	4	14	–	
Co II ratio	0	–	16	50	–	
Younger Brother (30 months)						6.6
% of normal	22	80	34	83	397	
CS ratio	6	36	9	21	–	
Co II ratio	15	–	24	57	–	
Younger Brother (37 months)						
% of normal	23	170	28	75	254	
CS ratio	9	67	11	29	–	
Co II ratio	13	–	16	43	–	–

Co I; complex I, Co II; complex II, Co III; complex III, Co IV; complex IV, CS; citrate synthase.
Enzyme activities are expressed as % of mean normal control activity relative to protein, relative to CS, and relative to Co II.

copy nuclear reference gene (exon 24 of the CFTR gene, chosen because it lacks single-nucleotide polymorphisms). For both experiments, DNA from six adult liver samples (from needle biopsies, obtained with informed consent) was used as controls. The results presented were the means of four independent runs, with samples assayed in triplicate in each run.

Mutation detection

Genomic DNA was extracted from liver or peripheral blood leukocyte according to the standard procedures. Detailed sequencing methods appear in the supplemental materials.

Results

Enzyme activities

Both affected siblings showed low activity levels of RC Co I, III, and IV. In particular, their Co I activities were strikingly low. In contrast, their Co II activities were maintained at normal, and those of citrate synthase were greatly elevated (Table 1). Co III and Co IV activity levels were higher in the younger brother than those in the elder brother.

BN-PAGE Western blot analysis

Fig. S2 shows the RC Co amounts by BN-PAGE in each brother. In both brothers, the band corresponding to either assembled Co I or assembled Co IV was invisible, and the band corresponding to the assembled Co III was strikingly weak. On the other hand, the intensity of the Co II band remained normal in both brothers.

Quantitative PCR

Quantitative PCR revealed that liver mtDNA was markedly decreased in both brothers (Table 1). The ratio of ND1 to CFTR in the liver of each brother was lower than those of the six controls (mean ± SD: 7.8 ± 4.6% for the elder brother, 6.6 ± 1.5% for the younger brother).

Mutations in MPV17

Both brothers were confirmed to be compound heterozygotes for c.451insC/c.509C > T (Fig. S3). c.451insC in exon 6 causes a frame-shift predicting an elongated gene product p.Leu151fsX189 (p.Leu151PhefsX39, according to the standard mutation nomenclature guidelines at http://www.genomic.unimelb.edu.au/mdi/mutnomen/). The c. 509C > T in exon 7 causes an amino acid substitution (Ser170Phe). These variations had not registered as genetic polymorphisms in the ensembl_mart_47 database (martdb.ensembl.org) and had not been reported as disease-causing mutations. Moreover, the alignment shows that both amino acid residues (Leu151 and Ser170) mutated in the affected siblings are absolutely conserved in all species (Fig. S4). Therefore, we consider these variations to be novel mutations. A single allele of c.451insC was present in all three siblings and their mother, whereas c. 509C > T was detected in both affected siblings and their father (Fig. S3). The fact that two such mutations were inherited from each parent independently indicated that these mutations were compound heterozygous in both affected siblings. The parents and the unaffected sibling had only one mutation, and had no obvious phenotype (Fig. S3). These observations support an autosomal recessive manner of inheritance for the hepatic dysfunction phenotype segregating within this family.

Discussion

Both brothers had novel compound heterozygous mutations, c.451insC/c.509C > T, but their clinical courses differed greatly. The phenotype of the elder brother was classified as possibly the infantile form, characterized by early onset liver disease that rapidly progresses to liver failure within the first few years of life [4,5].

In contrast, the younger brother exhibited a rather mild course. His liver damage was relatively mild, and he did not show any apparent neurological abnormality.

Such a great difference in the clinical courses between these brothers might be explained, in part, by the differences in their RC activity levels. The degree of reduction in RC activity was generally milder in the younger brother than in the elder. However, several studies have shown that RC activities were not correlated with the clinical course [4,5].

In our MPV17 mutant patients, the fluctuations in liver function were associated with infections that may cause oxidative stress. It was likely that cytomegalovirus infection promoted the onset and progression of liver disease in the elder brother, and that the liver dysfunctions in these siblings were greatly exacerbated by viral infections, in particular rotavirus infection.

Taken together, our experiences with these cases allowed us to assume that the clinical course and prognosis of MDS caused by MPV17 mutations were determined not only by the mutation but also by other factors. We postulated that many complicating factors may arise, including infection.

An effective treatment for mitochondrial RC disorders involving MDS has yet to be established. Liver transplantation is not so promising [6,12–14]. Besides the surgical complication, neurological regression after transplantation has been reported. Collectively, the survival rate is less than 50% [14].

For the younger brother, we tried to administer medications targeting the RC system, including succinate and coenzyme Q. Simultaneously, a lipid-rich carbohydrate-restricted diet using ketone milk was initiated. This combined treatment improved his liver disease biochemically and histologically. However, his liver RC activities did not improve.

Initially, he received a carbohydrate-rich, lipid-restricted diet and fat-soluble vitamins, together with UDCA, as had his elder brother. Recently, Parini et al. reported that glucose administration to avoid hypoglycemia is efficient in slowing the progression of liver disease [5]. However, this dietary treatment did not achieve favorable effects for our patients. Therefore, we resorted to another treatment for the younger brother.

The efficacy of medications with succinate and coenzyme Q, together with a lipid-rich diet, was possibly explained by their biochemical features. The mitochondrial RC system comprises Co I, II, III, and IV. Co I activity was markedly reduced in the younger brother, while his Co III activity remained mildly or moderately decreased. On the other hand, his Co II activity was entirely normal. Co I, an electron and proton acceptor from NADH and H^+, respectively, is the most important reduction-type hydrogen carrier, generating ATP by glucose oxidation [13]. From this context, glucose should hardly have been used as an energy source in the liver of the younger brother. On the other hand, succinate might donate electrons and protons to Co II connected to ubiquinone via $FADH_2$ [15]. In addition, a lipid-rich diet was expected to donate electrons and protons to ETF (electron-transfer flavoprotein): QO (ubiquinone oxidoreductase) connected to ubiquinone by promotion of $FADH_2$ production.

In summary, these cases suggested that the clinical course of MPV17 mutation is not determined solely by the mutation but rather is greatly influenced by viral infection, and that medications targeting Co II, together with a lipid-rich diet, may be beneficial in the clinical management of patients with MDS.

Acknowledgments

We acknowledge Kohda M. for helpful discussion. We also thank Hirata T. and Horiguchi N. for technical assistance. This work was supported by Grants-in-Aid for Scientific Research from the Japan Society for the Promotion of Science (16591052 and 19591220), by a Grant-in-Aid for the Development of New Technology from the Promotion and Mutual Aid Corporation for Private Schools of Japan, and by Saitama Medical University Internal Grant 06-015.

Appendix A. Supplementary data

Supplementary data associated with this article can be found, in the online version, at doi:10.1016/j.ymgme.2009.04.014.

References

[1] A. Spinazzola, C. Viscomi, E. Fernandez-Vizarra, F. Carrara, P. D'Adamo, S. Calvo, et al., MPV17 encodes an inner mitochondrial membrane protein and is mutated in infantile hepatic mitochondrial DNA depletion, Nat. Genet. 38 (2006) 570–575.
[2] E. Sarzi, A. Bourdon, D. Chrétien, M. Zarhrate, J. Corcos, A. Slama, et al., Mitochondrial DNA depletion is a prevalent cause of multiple respiratory chain deficiency in childhood, J. Pediatr. 150 (2007) 531–534.
[3] L.J. Wong, N. Brunetti-Pierri, Q. Zhang, N. Yazigi, K.E. Bove, B.B. Dahms, et al., Mutations in the MPV17 gene are responsible for rapidly progressive liver failure in infancy, Hepatology 46 (2007) 1218–1227.
[4] C.L. Karadimas, T.H. Vu, S.A. Holve, P. Chronopoulou, C. Quinzii, S.D. Johnsen, et al., Navajo neurohepatopathy is caused by a mutation in the MPV17 gene, Am. J. Hum. Genet. 79 (2006) 544–548.
[5] R. Parini, F. Furlan, L. Notarangelo, A. Spinazzola, G. Uziel, P. Strisciuglio, et al., Glucose metabolism and diet-based prevention of liver dysfunction in MPV mutant patients, J. Hepatol. 50 (2009) 215–221.
[6] S. Rahman, P.B. Blok, H.M. Dahl, D.M. Danks, D.M. Kirby, C.W. Chow, Leigh syndrome: clinical features and biochemical and DNA abnormalities, Ann. Neurol. 39 (1996) 343–351.
[7] D.M. Kirby, M. Crawford, M.A. Cleary, H.M. Dahl, X. Dennett, D.R. Tourburn, Respiratory chain complex I deficiency. An underdiagnosed energy generation disorder, Neurology 52 (1999) 1255–1264.
[8] F. Dabbeni-Sala, S. Di Santo, D. Franceschini, S.D. Skaper, P. Giusti, Melatonin protects against 6-OHDA-induced neurotoxicity in rats: a role for mitochondrial complex I activity, FASEB J. 15 (2001) 164–170.
[9] H. Schagger, H. Aquila, G. Von Jagow, Coomassie blue-sodium dodecyl sulfate-polyacrylamide gel electrophoresis for direct visualization of polypeptides during electrophoresis, Anal. Biochem. 173 (1988) 201–205.
[10] A.T. Pagnamenta, J.W. Taaman, C.J. Wilson, N.E. Anderson, R. Marotta, A.J. Duncan, Dominant inheritance of premature ovarian failure associated with mutant mitochondrial DNA polymerase gamma, Hum. Reprod. 21 (2006) 2467–2473.
[11] L. He, P.F. Chinney, S.E. Durham, E.L. Blakely, T.M. Wardell, G.M. Borthwick, et al., Detection, quantification of mitochondrial DNA depletions in individual cells by real-time PCR, Nucleic Acids Res. 30 (2002) e68.
[12] B. Dubern, P. Broue, C. Dubuisson, V. Cormier-Darie, C. Chardot, Orthotopic liver transplantation for mitochondrial respiratory chain disorders: a study of 5 children, Transplantation 71 (2001) 633–637.
[13] I. Trounce, Genetic control of oxidative phosphorylation and experimental models of defects, Hum. Reprod. 15 (2000) 18–27.
[14] W.S. Lee, R.J. Sokol, Mitochondrial hepatopathies: advances in genetics and pathogenesis, Hepatology 45 (2007) 1555–1565.
[15] D.R. John, Mitochondrial DNA and disease, N. Engl. J. Med. 333 (1995) 638–644.

Cancer Chemother Pharmacol (2010) 65:251–258
DOI 10.1007/s00280-009-1029-2

ORIGINAL ARTICLE

Association of *UGT2B7* and *ABCB1* genotypes with morphine-induced adverse drug reactions in Japanese patients with cancer

Ken-ichi Fujita · Yuichi Ando · Wataru Yamamoto · Toshimichi Miya · Hisashi Endo · Yu Sunakawa · Kazuhiro Araki · Keiji Kodama · Fumio Nagashima · Wataru Ichikawa · Masaru Narabayashi · Yuko Akiyama · Kaori Kawara · Mari Shiomi · Hiroyasu Ogata · Hiroyasu Iwasa · Yasushi Okazaki · Takashi Hirose · Yasutsuna Sasaki

Received: 23 January 2009 / Accepted: 4 May 2009 / Published online: 23 May 2009

Abstract
Purpose To investigate the effects of genetic polymorphisms on morphine-induced adverse events in cancer patients.
Methods We examined the relation of morphine-related adverse events to polymorphisms in *UDP-glucuronosyltransferase (UGT) 2B7*, *ATP-binding cassette, sub-family B, number 1 (ABCB1)*, and *μ-opioid receptor 1* genes in 32 Japanese cancer patients receiving oral controlled-release morphine sulfate tablets.
Results The T/T genotype at 1236 or TT/TT diplotype at 2677 and 3435 in *ABCB1* was associated with significantly lower frequency of fatigue (grades 1–3) ($P = 0.012$ or 0.011, Fisher's exact test). The *UGT2B7*2* genotype was associated with the frequency of nausea (grades 1–3) ($P = 0.023$). The frequency of nausea was higher in patients without *UGT2B7*2* allele than others. The diplotype at 2677 and 3435 in *ABCB1* was associated with the frequency of vomiting (grades 1–3) ($P = 0.011$). No patient whose diplotype was consisted of no GC allele at 2677 and 3435 suffered from vomiting.
Conclusion Our findings suggest that pharmacogenetics can be used to predict the risk of morphine-induced adverse events.

Keywords Morphine · Cancer patients · Adverse reaction · Pharmacogenetics

K. Fujita (✉) · Y. Ando · W. Yamamoto · T. Miya · H. Endo · Y. Sunakawa · K. Araki · K. Kodama · F. Nagashima · W. Ichikawa · M. Narabayashi · Y. Akiyama · K. Kawara · T. Hirose · Y. Sasaki
Department of Medical Oncology, Saitama International Medical Center-Comprehensive Cancer Center, Saitama Medical University, 1397-1 Yamane, Hidaka, Saitama 350-1298, Japan
e-mail: fujitak@saitama-med.ac.jp

K. Fujita · F. Nagashima · Y. Akiyama · Y. Sasaki
Project Research Laboratory, Research Center for Genomic Medicine, Saitama Medical University, 1397-1 Yamane, Hidaka, Saitama 350-1241, Japan

M. Shiomi · H. Ogata
Department of Biopharmaceutics, Meiji Pharmaceutical University, 2-522-1 Noshio, Kiyose, Tokyo 204-8588, Japan

H. Iwasa · Y. Okazaki
Division of Translational Research, Research Center for Genomic Medicine, Saitama Medical University, 1397-1 Yamane, Hidaka, Saitama 350-1241, Japan

Introduction

Severe pain caused by tumors is therapeutically managed by administration of opioid analgesics. Morphine is one of the most important and widely used opioids for cancer-pain relief, but large interindividual variability in its effectiveness and adverse reactions are a major clinical disadvantage. Clinical pharmacology studies have demonstrated that wide interindividual variability in the response to a drug is associated with considerable pharmacokinetic or pharmacodynamic variability [1], which may be genetically determined [2–4].

Morphine is predominantly glucuronidated by UDP-glucuronosyltransferase (UGT) 2B7 to form morphine 6-glucuronide (M6G) and morphine 3-glucuronide (M3G) [5]. M6G has clinically been shown to be a potent analgesic, and the analgesic properties of morphine are enhanced

by the action of M6G [6]. In contrast, M3G decreases the analgesic activity of morphine and M6G [6]. Therefore, polymorphisms in the *UGT2B7* gene are associated with interindividual variability in the pharmacokinetics of morphine and its metabolites. Although the effects of genetic polymorphisms in *UGT2B7* on the pharmacokinetics of morphine and its efficacy in patients with cancer have been reported [7, 8], whether such polymorphisms influence morphine-related adverse reactions remains unclear.

Efflux transporter P-glycoprotein [ATP-binding cassette, sub-family B, member 1 (ABCB1)], coded by the *ABCB1* gene, is a major determinant of the intracellular concentration of morphine and its metabolites, M6G and M3G [9]. ABCB1 can limit the entry of morphine and its metabolites into the brain and actively pump the drug out of the central nervous system. It is thus an important component of the blood–brain barrier [10]. So far, a variety of polymorphisms in the *ABCB1* gene have been identified [11]. Recently, Campa et al. [12] have shown that pain-relief variability in patients with cancer is significantly associated with 3435C > T in the *ABCB1* gene. This finding suggests that genetic variability of *ABCB1* may affect morphine disposition in the central nervous system. However, few studies have examined the relation between *ABCB1* genetic polymorphisms and morphine-induced adverse drug reactions in patients with cancer who receive morphine.

The primary site of action of morphine is the μ-opioid receptor, which is encoded by the *opioid receptor μ1* (*OPRM1*) gene. *OPRM1* is thus an initial candidate gene for studies evaluating the role of polymorphisms in the clinical response to morphine. A variety of polymorphisms have been identified in the *OPRM1* gene [13, 14]. The most prevalent polymorphism in the *OPRM1* gene is a nucleotide substitution 118A > G, causing amino acid change N40D at a putative *N*-glycosylation site in the extracellular region of the receptor. Recently, 118A > G was demonstrated to lower mRNA and functional protein expression in human brain tissue and in transfected cells [15]. To date, the association between single nucleotide polymorphism (SNP) and the efficacy of morphine has been relatively well investigated. Cancer patients homozygous for the G allele were found to be poor responders to morphine [12] and to require higher doses of morphine to relieve pain [16]. However, the association between 118A > G in *OPRM1* and morphine-induced adverse reactions in patients with cancer remains unclear.

We examined the effects of polymorphisms in the *UGT2B7*, *ABCB1*, and *OPRM1* genes on morphine-related adverse reactions in patients with cancer who received morphine therapy.

Methods

Materials

Morphine hydrochloride was kindly provided by Shionogi (Osaka, Japan). M3G, M6G, and naloxone hydrochloride were purchased from Sigma-Aldrich (St. Louis, MO, USA). All chemicals and solvents were of the highest grade commercially available.

Patients

Japanese patients with cancer who were receiving controlled-release morphine sulfate tablets (MS Contin, Shionogi, Osaka, Japan) to relieve cancer pain were enrolled. The protocols for the pharmacokinetic study of morphine and its metabolites and the pharmacogenetic study were approved by the Institutional Review Board of Saitama Medical University. All patients gave written informed consent for their peripheral blood samples and medical information to be used for research purposes.

Treatments

Controlled-release morphine sulfate tablets were orally administered to patients according to the standard protocol described in the package insert. When the initial dose was appropriate to relive pain, the dose was determine as maintenance dose. If necessary, the initial morphine dose was modified to achieve the pain relief. When the pain was relieved enough by the modification of dose, the dose was determined as the maintenance dose. If patients did not tolerate with morphine treatment because of adverse events, the dose was adopted as maintenance dose. Thus, maintenance dose depended on the pain intensity of the patients and susceptibility of them to morphine. When the maintenance dose was obtained, morphine-induced adverse events were evaluated.

Morphine-induced adverse reactions

Morphine-induced adverse events, including constipation, nausea, vomiting, drowsiness/confusion, and fatigue, were evaluated according to the National Cancer Institute Common Toxicity Criteria (NCI-CTCAE), Version 3.0.

Genotyping

Genomic DNA was extracted from 200 μl of peripheral blood, which had been stored at −80°C until analysis, with the use of a QIAamp Blood Kit (QIAGEN GmbH, Hilden, Germany).

UGT2B7 gene fragments containing 211G > T [rs12233719, A71S] and 802C > T [rs7439366, H268Y,

*UGT2B7**2] were amplified by polymerase chain reaction (PCR). Genomic DNA samples (100 ng) were added to the PCR mixtures (50 μl), consisting of 1× PCR buffer, 3 mM $MgCl_2$ for 211G > T or 4 mM $MgCl_2$ for *2, 0.25 μM of each primer, 200 μM dNTPs, and 1.25 U of AmpliTaq Gold DNA polymerase (Applied Biosystems, CA, USA). The PCR primers used to amplify the *UGT2B7* gene fragments containing the respective polymorphisms were 2B7A71S-F (5′-TTAGTTTTGTGTCAATGGACTGCAGAAAC-3′) and 2B7A71S-R (5′-AAATAAGTTAGAGCTTCATGTTACT GATTG-3′) for 211G > T, and 2B7*2-F (5′-CTGTCAG GAAGACCCACTAC-3′) and 2B7*2-R (5′-TTTACCTTA GGCAGGGGTTT-3′) for 802C > T. All amplifications included a 15-min initial denaturation at 94°C. PCR was performed under the following conditions: 30 s at 94°C (40 s for *2), 40 s at 57°C (30 s at 56°C for *2), and 1 min at 72°C for 211G > T (30 s for *2) for 30 cycles, followed by a final extension at 72°C for 3 min. After the purification of the PCR products with QIAquick PCR purification kit (QIAGEN GmbH, Hilden, Germany), direct sequencing was performed with BigDye terminator var. 3.1 cycle sequencing kit and on a 3130 genetic analyzer (Applied Biosystems, CA, USA).

Gene fragments of *ABCB1* that included 1236C > T [rs1128503, G412G], 2677G > T, A [rs2032582, A893T, S], and 3435C > T [rs1045642, I1145I] were amplified by PCR. Forward and reverse primers used for PCR to amplify *ABCB1* gene fragments containing these polymorphic sites were ABCB1-1236F (5′-TGAATGAAGAGTTTCTGATGT TTTCTTG-3′) and ABCB1-1236R (5′-ATACATTTGTAAT TGAAAGGGCAACAT-3′), ABCB1-2677F (5′-AATGAAT ATAGTCTCATGAAGGTGAGTTTT-3′) and ABCB1-2 677R (5′-CATTCTTAGAGCATAGTAAGCAGTAGGG-3′), and ABCB1-3435F (5′-TGGCAGTTTCAGTGTAAGAAA TAATGA-3′) and ABCB1-3435R (5′-TAATTTCTCTTCA CTTCTGGGAGACC-3′), respectively. PCR was carried out in a total volume of 50 μl in the presence of 100 ng of genomic DNA, 0.25 μM each primer, 1× PCR buffer, 3 mM $MgCl_2$, 0.2 mM dNTPs, and 1.25 U of AmpliTaq Gold DNA polymerase. An initial denaturation at 94°C for 15 min was followed by 30 cycles of 0.5 min at 94°C, 40 s at 62°C, and 40 s at 72°C, as well as a final extension period of 3 min at 72°C. PCR products were sequenced directly as described above.

OPRM1 gene fragment containing 118A > G [rs17999 71, N40D] was amplified by means of PCR. The forward and reverse primers used were 5′-TTTCCCTCCTCCCTCC CTTC-3′ and 5′-GCCTTGGGAGTTAGGTGTCTCTTT-3′, respectively. Genomic DNA samples (100 ng) were added to the PCR mixtures (50 μl) consisting of 1× PCR buffer, 4 mM $MgCl_2$, 0.25 μM of each primer, 200 μM dNTPs, and 1.25 U of AmpliTaq Gold DNA polymerase. Amplification was performed by denaturation at 95°C for 30 s, annealing at 61°C for 40 s, and extension at 72°C for 1 min for 30 cycles, followed by a final extension at 72°C for 3 min. PCR products were subsequently directly sequenced as mentioned above.

Determination of morphine, M6G, and M3G

Blood samples for pharmacokinetic analysis were obtained after oral administration of morphine. A blood sample was arbitrarily obtained during the period between one dose of morphine and the next dose. The samples were centrifuged immediately, and resulting plasma samples were stored at −80°C until analysis.

Plasma concentrations of morphine, M6G, and M3G were analyzed by reverse-phase high-performance liquid chromatography (HPLC). The HPLC system consisted of an EP-300 pump, ATC-300 column thermostat, EP-300 electron chemical detector (ECD), DG-300 degasser (Eicom, Kyoto, Japan), SIL-20A auto-sampler, SPD-10AVVP ultraviolet (UV) detector, and C-R6A Chromatopac (Shimadzu, Kyoto, Japan).

Morphine and M6G were analyzed with the use of an ECD and a SuperODS column (4.6 × 100 mm, 2.3 μm; Tosoh, Tokyo, Japan). The oxidation potential was 750 mV. The mobile phase was a mixture of 0.1 M phosphate buffer (pH 2.1) containing 30 μM EDTA and 10 mM sodium dodecyl sulfate, acetonitrile, and methanol at a ratio of 90:8:2 (v/v). The column temperature was 40°C and the flow rate was 1.0 ml/min.

M3G was analyzed with the use of a UV detector and an L-column ODS (4.6 × 250 mm, 5 μm; Chemicals Evaluation and Research, Saitama, Japan). The wavelength of the UV detector was 210 nm, and the column temperature was 40°C. The mobile phase consisted of 0.1 M phosphate buffer (pH 2.1) containing 30 μM EDTA and 10 mM sodium dodecyl sulfate, acetonitrile, and methanol at a ratio of 74:24:2 (v/v) and was delivered at a flow rate of 1.0 ml/min.

The lower limits of quantification were 67.2 pg/ml (236 pM) for morphine, 380 pg/ml (0.823 nM) for M6G, and 496 pg/ml (1.08 nM) for M3G.

Pharmacokinetic parameters

Individual oral clearances (l/h) of morphine were estimated by empirical Bayes estimates, based on a prior non-linear mixed effect analysis fit, using a 1-compartment model. Non-linear mixed effect analysis was performed with NONMEM program version VI (Globemax LLC, Hanover, MD, USA) to develop a population pharmacokinetic model.

Statistical analysis

Genotype and allele frequencies for each polymorphic allele in the respective genes were determined by using

SNPAlyze 5.1 (Dynacom, Yokohama, Japan). The significance of deviations from Hardy–Weinberg equilibrium was also tested with the program SNPAlyze 5.1. Linkage disequilibrium analysis to create a pairwise two-dimensional map of correlation coefficients r^2 and D' among SNPs in the *ABCB1* gene was performed with SNPAlyze 5.1. Relations between the morphine maintenance dose and morphine-induced adverse reactions were evaluated with the use of Spearman's rank correlation coefficient. The Fisher's exact test were employed to analyze the association of *UGT2B7*, *ABCB1*, and *OPRM1* diplotypes or genotypes with morphine-related adverse events as graded by NCI-CTCAE, ver. 3.0 (grade 0 versus other) (JMP version 6 software, SAS Institute, Inc., Cary, NC, USA). A *P*-value of less than 0.05 was considered to indicate a statistically significant difference.

Results

Patient characteristics and morphine-induced adverse reactions

A total of 32 Japanese patients with cancer who received controlled-release morphine sulfate were enrolled in this study from July 2006 through February 2007. The patient characteristics are summarized in Table 1. The most frequent tumor was breast cancer, followed by colorectal and pancreatic cancers. Most patients (29/32) had metastases to various organ(s). Renal function evaluated on the basis of the serum creatinine level was normal in all patients.

Table 1 Patient characteristics

Characteristics	Values	Number of patients
Age (years)[a]	64.5 (38–77)	32
Sex (male/female)		15/17
Serum creatinine (mg/dl)[a]	0.7 (0.5–1.2)	32
Total bilirubin (mg/dl)[a]	0.4 (0.2–14.4)	32
Tumor type		
Breast		8
Colorectal		7
Pancreas		4
Stomach		3
Esophagus		3
Others		7
Maintenance dose (mg/day)	20/30/40/60/80	21/3/3/4/1
Metastasis		
	Yes/no	29/3

[a] Values are expressed as medians, with ranges in parentheses

Hepatic function estimated on the basis of the total bilirubin level was normal in all but one patient, who had a value of 14.4 mg/dl. Morphine-induced adverse reactions are shown in Table 2. There was no relation between the maintenance dose of morphine and the respective morphine-induced adverse reactions (Spearman's rank correlation coefficient).

Genotype and allele frequencies of polymorphisms in *UGT2B7*, *ABCB1*, and *OPRM1* genes

The genotype and allele frequencies of polymorphisms in the *UGT2B7*, *ABCB1*, and *OPRM1* genes are shown in Table 3. Allele frequencies of polymorphisms in the *UGT2B7* and *ABCB1* genes were roughly equal to those previously reported [7, 11]. The genotype and allele frequencies of 118A > G in the *OPRM1* gene were consistent with the HapMap data reported for Japanese (http://www.ncbi.nlm.nih.gov/SNP/snp_ref.cgi?rs=1799971). All polymorphisms were in Hardy–Weinberg equilibrium ($P > 0.05$). We found that 3435C > T in the *ABCB1* gene was strongly linked to 2677G > T ($r^2 = 0.711$ and $D' = 0.927$), but not to 1236C > T, although Sai et al. [17] demonstrated linkage among 1236C > T, 2677G > T, and 3435C > T.

UGT2B7, *ABCB1*, and *OPRM1* genotypes and morphine-induced adverse reactions

The *UGT2B7*2* genotype was significantly associated with the frequency of nausea (grades 1–3; $P = 0.023$; Fig. 1). The frequency of nausea was higher in patients without *UGT2B7*2* allele than others. However, the systemic oral clearance of morphine did not differ significantly between the two groups of genotype, without *UGT2B7*2* and at least one *UGT2B7*2* allele. The frequency of other adverse reactions were also slightly higher in patients without *UGT2B7*2* than in those with at least one *UGT2B7*2* allele. A71S mutation was not related to any type of morphine-induced adverse events or to morphine clearance.

The genotype at 1236 in *ABCB1* gene was associated with the frequency of fatigue (grades 1–3; $P = 0.012$;

Table 2 Morphine-induced adverse reactions

Adverse reactions	Grade	Numbers of patients
Constipation	0/1/2/3	15/12/4/1
Nausea	0/1/2/3	21/7/3/1
Vomiting	0/1/2/3	25/3/1/1
Drowsiness/confusion	0/1/2/3	22/1/9/0
Fatigue	0/1/2/3	18/7/6/1

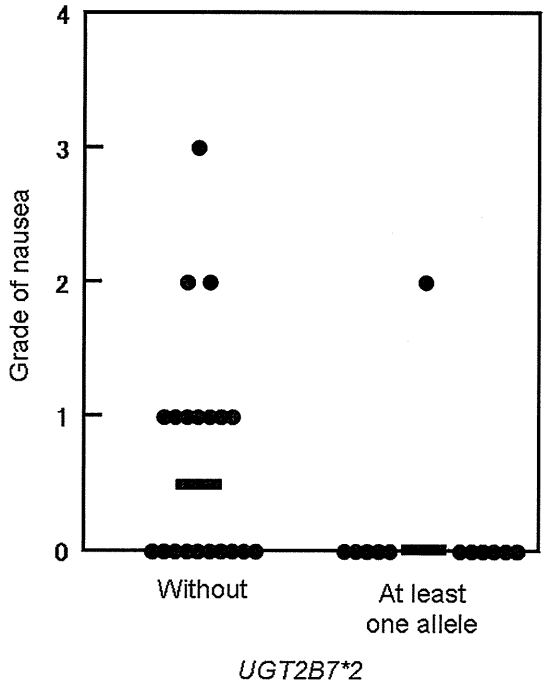

Fig. 1 *UGT2B7*2* genotype and morphine-induced nausea. Bars indicate medians

Fig. 2). The frequency of fatigue in patients with the T/T genotype at 1236 was significantly lower than that with other genotypes. The frequency of fatigue (grades 1–3) was also significantly lower in patients with TT/TT diplotype at 2677 and 3435 in *ABCB1* gene than in other patients ($P = 0.011$; Fig. 2). Morphine oral clearance was slightly but not significantly higher in patients with T/T genotype at 1236 or TT/TT diplotype at 2677 and 3435 than in other patients ($P = 0.103$ and 0.116, Mann–Whitney *U*-test). The diplotype at 2677 and 3435 in *ABCB1* was associated with the frequency of vomiting (grades 1–3; $P = 0.011$; Fig. 3). No patient without GC allele at 2677 and 3435 suffered from vomiting. The frequency of nausea (grades 1–3) in patients without GC allele at 2677 and 3435 in *ABCB1* was tended to be lower than others ($P = 0.061$). The oral clearance of morphine, M6G, and M3G did not differ significantly between these groups.

Morphine-induced adverse reactions were not associated with the polymorphism of 118A > G in the *OPRM1* gene.

The maintenance dose of morphine did not differ significantly between any two groups divided according to genotypes or diplotype for any of the adverse reactions described above.

Discussion

Our study showed that the grade of morphine-related adverse reactions was associated with genetic polymorphisms in genes

Table 3 Genotype and allele frequencies of polymorphisms in the *UGT2B7*, *ABCB1*, and *OPRM1* genes

	Polymorphism	Genotype	Number (frequency)	Allele	Frequency
UGT2B7	−327G > A	G/G	17 (0.53)	G	0.70
		G/A	11 (0.34	A	0.30
		A/A	4 (0.13)		
	211G > T	G/G	29 (0.91)	G	0.95
		G/T	3 (0.09)	T	0.05
		T/T	0 (0)		
	802C/T	C/C	20 (0.62)	C	0.75
		C/T	8 (0.25)	T	0.25
		T/T	4 (0.13)		
ABCB1	1236C > T	C/C	5 (0.16)	C	0.38
		C/T	14 (0.43)	T	0.62
		T/T	13 (0.41)		
	2677G > T, A	G/G	6 (0.19)	G	0.39
		G/T	9 (0.28)	T	0.45
		G/A	4 (0.13)	A	0.16
		T/A	4 (0.13)		
		T/T	8 (0.24)		
		A/A	1 (0.03)		
	3435C > T	C/C	7 (0.22)	C	0.5
		C/T	18 (0.56)	T	0.5
		T/T	7 (0.22)		
OPRM1	118A > G	A/A	7 (0.22)	A	0.48
		A/G	17 (0.53)	G	0.52
		G/G	8 (0.25)		

that encode factors related to morphine pharmacokinetics and pharmacodynamics, including *UGT2B7*, *ABCB1*, and *OPRM1*.

The frequency of nausea was higher in patients without *UGT2B7*2* allele than others (Fig. 1); the systemic oral clearance of morphine did not differ significantly between the two groups. Coffman et al. [18] have demonstrated that UGT2B7.2 is capable of catalyzing morphine to inactive M3G more efficiently than to active M6G. Therefore, morphine might be detoxified more rapidly in patients with *UGT2B7*2* than in other patients, supporting our results that the incidence of morphine-induced adverse events was lower in patients with *UGT2B7*2*.

In our study, the T/T genotype at 1236 or TT/TT diplotype at 2677 and 3435 in *ABCB1* was associated with significantly lower frequency of fatigue (Fig. 2). This difference might be attributed to lower systemic exposure to morphine in patients homozygous for T allele at 1236 or TT/TT diplotype at 2677 and 3435. This notion is supported by the fact that morphine oral clearance in patients

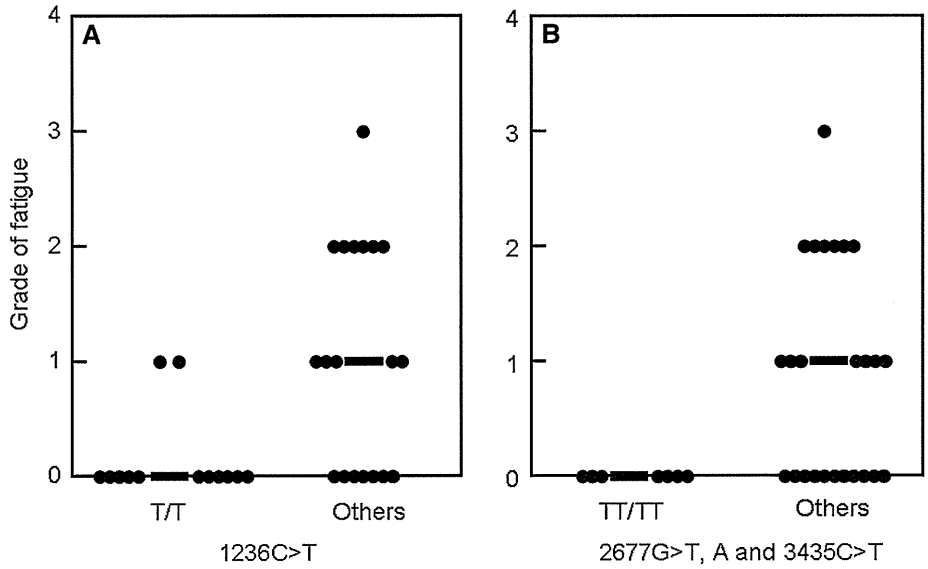

Fig. 2 *ABCB1* genotype or diplotype and morphine-related fatigue **a** 1236C > T, **b** 2677C > T, A and 3435C > T. Bars represent medians

with T/T genotype at 1236 or TT/TT diplotype at 2677 and 3435 tended to be higher than that in other patients. However, Meineke et al. [19] showed that the TT genotype of 3435C > T is associated with lower ABCB1 expression. To date, the functional effects of 1236C > T, 2677G > T, A, and 3435C > T in the *ABCB1* gene on the pharmacokinetics, efficacy, and adverse events of drugs remain controversial [20–32]. Further studies are necessary to elucidate the roles of these polymorphisms on the functions of ABCB1.

The frequency of vomiting was significantly higher in patients with one GC allele at 2677 and 3435 than in other patients (Fig. 3). In contrast, Coulbaut et al. [33] demonstrated that the GC/GC diplotype at 2677 and 3435 in the *ABCB1* gene was significantly associated with lower incidences of morphine-related nausea and vomiting as evaluated by the use of ondansetron. The results of these studies do not agree with our findings. One reason for the discrepancy may the difference in the administration route of morphine. In our study, morphine was administered orally, whereas in the study by Coulbaut et al. [33], morphine was administered intravenously to control postoperative pain. Since orally administered morphine is subject to the actions of ABCB1 expressed in the small intestine, the effects of polymorphisms in the *ABCB1* gene on pharmacokinetics might differ between intravenously and orally administered morphine.

Although Campa et al. [12] have shown that pain-relief variability in patients with cancer is significantly associated with 3435C > T in the *ABCB1* gene, they have not found any relations between morphine-induced adverse events and *ABCB1* polymorphisms, which was inconsistent with our present results.

Morphine-induced adverse reactions were not associated with the polymorphism of 118A > G in the *OPRM1* gene. As reported previously, cancer patients homozygous for the

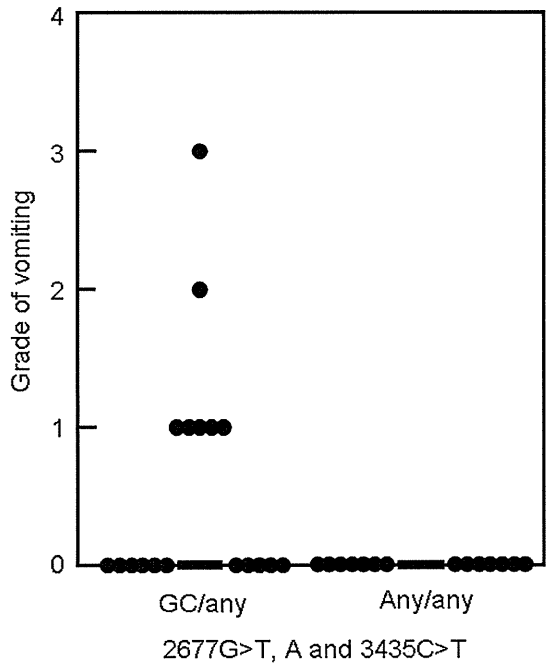

Fig. 3 *ABCB1* diplotype and morphine-induced vomiting. Bars represent medians

G allele were found to be poor responders to morphine [12] and to require higher doses of morphine to relieve pain [16]. These findings suggest that morphine-related adverse reactions are likely to occur in patients with G allele at 118, given that the mechanism of morphine-induced adverse events involves OPRM1. However, our results do not support this notion. Further analysis is necessary to confirm whether morphine-induced fatigue is directly related to the function of OPRM1.

It has been reported that V158M in catechol-*O*-methyl transferase (COMT) is associated with the response of morphine and further with morphine dose requirement [34]. We